JOURNAL OF ADVANCED INDUSTRIAL TECHNOLOGY AND APPLICATION
e-ISSN: 2716-7097

JAITA

Vol. 6 No. 1 (2025) 112-126
https://publisher.uthm.edu.my/ojs/index.php/jaita

Taguchi-Grey Optimisation of TIG Welding Parameters and its Impact on the Mechanical Properties of Austenitic Steel

Afabor A. Martins[1]*, Onyekpe B[2], Awheme Oghenerobo[2]

[1] *Department of Materials and Metallurgical Engineering, Delta State University of Science and Technology, Ozoro, NIGERIA*
[2] *Department of Materials and Metallurgical Engineering, University of Benin, Benin City, NIGERIA*

*Corresponding Author: afabormartins2@gmail.com
DOI: https://doi.org/10.30880/jaita.2025.06.01.10

Article Info

Received: 25 Oktober 2024
Accepted: 17 March 2025
Available online: 30 June 2025

Keywords

Austenitic, steel, welding, TIG, optimisation, Taguchi-Grey

Abstract

Welding, albeit tungsten inert gas welding; is a unique and widely adopted joining process especially for austenitic stainless steel arising from its advantages over other welding process. However very often, mechanical properties and weld quality could be deteriorated if the weld parameters are not controlled during a welding operation. Selecting the appropriate process parameters for welding operations is crucial for forming weld microstructures with excellent mechanical properties, thereby enhancing weldment performance during service. Thus in this study, the integrated Taguchi-Grey optimisation technique has been adopted in the optimisation of welding parameters. The Taguchi L27 orthogonal array design of experiment consisting of three levels of four factors of current, voltage, speed and gas flowrate was deployed for the determination of multi performance index for the output parameters of tensile strength and microhardness. The results obtained, after a confirmatory test to validate the predictive model indicates that there was an improvement from 0.0409 to 0.495 in MRPI, for the optimal parameters setting of current at 95 A, speed at 0.7 mm/s, voltage at 25 V and gas flow rate at 20 L/min respectively. This study could influence industrial practices by improving weld quality, reducing material wastage, and enhancing process efficiency. For example, optimizing welding parameters can minimise defects in aerospace applications or lead to stronger, lighter components in automotive manufacturing, improving both safety and performance. Potential cost savings could also be achieved from optimised parameter selection and reduced trial and-error approaches in industrial applications. This methodology can also be adapted to other materials or welding techniques like friction stir welding or laser welding.

1. Introduction

TIG welding is a popular welding method for combining austenitic stainless steel grades. Weld quality enhances mechanical qualities and corrosion resistance, leading to longer component life and fewer unexpected failures. Controlling weld parameters during welding can prevent mechanical and corrosion qualities from deteriorating.

Austenitic stainless steel, also referred to as the 300 series, presents unique difficulties when joined with tungsten inert gas welding, the most challenging of which are carbide precipitation and deformation. Austenitic stainless steel is more likely to warp than mild steel due to its increased susceptibility to heat expansion- roughly

50% more so than mild steel. Austenitic steel has a low heat conductivity, which causes buckling when the weld cools and slows the transfer of heat to the surrounding material. These issues can be caused by an insufficient gas flow rate, an excessively slow or fast travel speed, or an excessive welding current setting. Thus, if the welding parameter settings are not chosen appropriately, the weld will have the aforementioned welding flaws [1]. Optimising the parameters of GTAW is important as it can lead to improved mechanical properties of welded joints, such as increased strength and reduced defect rates. This can ultimately enhance the overall quality and reliability of welded structures.

The Taguchi's design of experiments identifies the optimal parameters for the process while minimising the number of experimental trials required. The Taguchi method is used to optimise welding parameters for single weld properties; it doesn't work well in the case of multiple weld properties [2]. The conventional Taguchi method is not capable of efficiently and effectively addressing multi-objective optimisation problems. Consequently, the optimisation performance attributes are effectively managed by the integrated Taguchi-Grey relational analysis, which the Taguchi technique alone could not do [3]. The combined Taguchi-based Grey relational analysis optimisation approach was employed to address this restriction. The suggested technique effectively selects optimal parameters for particle swarm optimisation using fewer data sets, as demonstrated by the results.

Grey relational analysis has been applied by several researchers [4,5] to optimise the control parameters having multi-responses through grey relational grade. A study by [6] examined the optimisation and implementation elements of Taguchi-Grey relational analysis in the identification of appropriate PSO parameters for manufacturing-related issues. The results show the effectiveness of the proposed approach in selecting the optimum parameters for particle swarm optimisation by considering a smaller number of data sets.

2. Analysis Techniques

2.1 Taguchi Design of Experiment

The Taguchi approach is an easy and cost-effective method of obtaining process optimisation with strong quality and performance, which greatly reduces the range of experiments needed [7] and offers a relevant correlation between input and output parameters [8]. This study used a Taguchi L27 orthogonal array with three levels of four input parameters: welding current, welding speed, welding voltage, and shielding gas flow rate (see Table 1).

These parameter ranges reflect practical conditions in welding operations of austenitic steels and they align with prior studies conducted [1, 9 - 11], demonstrating effective heat input and weld quality control. However including additional levels or parameters could enhance the robustness of the optimisation process, revealing nonlinear trends or interactions that might be missed. Also the incorporating external factors, such as environmental conditions, humidity, vibration or temperature as well as welding expertise could lead to improved process robustness, increased efficiency and enhanced product quality which would results in improved resilience and applicability of the methodology.

Table 1 *GTA welding parameters and their Levels*

No.	Parameters	Code	Unit	Level 1 (Low)	Level 2 (Medium)	Level 3 (High)
1	Current	J	Ampere (A)	95	100	105
2	Speed	K	mm/s	0.7	0.9	1.1
3	Voltage	L	Volt (V)	23	25	27
4	Gas flow rate	M	Litre per minute (L/min.)	10	15	20

2.2 Calculation of Signal-to-Noise Ratios (SNR)

Optimal signal-to-noise (SNR) ratios include larger-the-better, smaller-the-better, and nominal the best. To maximise responsiveness, the larger-the-better SNR is employed, with bigger values indicating better performance.The tensile strength and microhardness are a larger-the-better performance characteristic since the maximisation of the quality characteristic of interest is sought and can be expressed as Equation 1 [9, 12, 13].

$$SNR = -10\ log\left(\sum_{i=1}^{n} \frac{y_i^{-2}}{n}\right) \quad (1)$$

Where n = number of replications, y = observed value, and i = 1, 2, *n*,
SNR nominal-the-best is used when the goal of response optimisation is the target response.

2.3 Grey Relational Analysis

Grey's relational technique is used to analyse four welding factors (current, speed, voltage, and gas flow rate) at three levels, with tensile strength and microhardness as output parameters.

Step 1: Involves normalising all experimental findings to a range of zero (0) to one (1), also known as data normalisation.
Step 2: In this experimental investigation, stronger tensile strength and hardness criteria were used.
Step 3: calculates the grey relational coefficient (GRC).
Step 4: The grey relational grade (GRG) is computed.

2.3.1 Normalisation of Signal-to-Noise Ratios

Signal-to-noise ratios are normalised into three categories based on their predicted response values. This study aims to achieve greater micro-hardness and tensile strength. The 'greater the better' normalisation criteria is used for micro-hardness and tensile strength. Also, it is necessary to normalise the calculated SNR ratio values before proceeding for the analysis. The formula for the 'higher the better' normalisation criteria considered is as presented in Equation 2 [14]:

$$x_j(n) = \frac{y_j(n) - y_{j_{(min.)}}}{y_{j_{(max.)}} - y_{j_{(min.)}}} \quad (2)$$

$x_j(n)$ = Normalised Grey relational value
$y_{j_{(min.)}}$ = lowest value of $y_j(n)$ for the nth response
$y_{j_{(max.)}}$ = highest value of the $y_j(n)$ for the nth response
Accordingly, the normalised values of the responses are calculated and presented in Table 2.

2.3.2 Grey Relational Coefficients (GRCs)

Calculate the grey relational coefficient (GRC) for each target and reference value on their respective elements. The GRCs on the normalised SNR values can be calculated as per Equation 3 [15]. The results so obtained are presented in Table 3.

$$\Gamma_j(n) = \frac{\Delta_{min.} + \xi\Delta_{max.}}{\Delta_j(n) + \xi\Delta_{max.}} \quad (3)$$

Where $\Gamma_j(n)$ = Grey relational coefficient

$\Delta(n)$ represents the absolute difference between the goal value $x0$ and the reference value $xj(n)$.
$\Delta min.$ is the absolute value of the minimal difference between the goal and reference values.
Δmax represents the absolute magnitude of the largest difference between the goal and reference values.
ξ = 0.5, is the resolution coefficient (between 0 and 1), usually takes a value of 0.5.

Normalisation transforms the responses into a common scale usually between 0 and 1, thereby eliminating difference in units, allowing responses with different units to be compared directly. Calculations of Grey relational coefficients help to assign relative importance to each response, reflecting their significance in the optimisation process. Normalisation and coefficient calculations ensures fair comparisons across responses in multi response optimisation process, thereby addressing potential biases.

2.3.3 Grey Relation Grade

The Grey relation grade (n) is calculated by taking the arithmetic mean of the GRCs between target and reference value answers. This number represents the degree of correlation between the reference value and the assessment aim. The Grey relation grade is calculated as per Equation 4 [16].

$$\gamma_j(n) = \frac{1}{m}\sum_{n=1}^{m}\Gamma_j(n) \quad (4)$$

When each response data has different weights in the comprehensive evaluation, it is necessary to consider the weight coefficient of the response to get the weighted average (W_n) value in solving the GRG as per Equation 5 [12].

$$\gamma_j(n) = \frac{1}{m}\sum_{n=1}^{m} W_n \,.\Gamma_j(n), \quad \sum_{n=1}^{m} W_n = 1 \quad (5)$$
$$n = 1, 2, \ldots, m$$

Where W_n is the given weight to the nth factor and m is the number of response characteristics.

Weights of 0.6 and 0.4 were assigned to the grey relationship coefficients of tensile strength and microhardness respectively. Higher weight was assigned to tensile strength, highlighting tensile strength's role in structural integrity and load-bearing applications. For example, tensile strength ensures safety in structural applications, while microhardness enhances surface wear resistance. The correlation degree between the goal and reference values is graded. A higher correlation degree indicates more consistent change between the two values.

3. Materials and Methods

3.1 Materials and Equipment

The GTAW equipment used in this study for welding the AISI 316L steel (with the chemical composition as shown in Table 2 was a DC argon arc welding machine (Miller Gold Star 602) as shown in Fig. 1. AISI 316L steel was chosen for this study as it has excellent corrosion resistance, high mechanical strength, and weldability, making it ideal for applications in harsh environments such as chemical processing and marine industries. ER 316 filler wire of diameter 3.2 mm was selected for this experiment as depicted in Fig. 2, and its elemental chemical composition is as stated in Table 2. ER316L filler material complements the base material, ensuring consistent weld properties and minimising issues like galvanic corrosion. ASTM-standard tensile test samples with their weld bead located at the centre of each sample were prepared. Experimental test samples (UTS and hardness) used for this study are displayed in Figs. 3a and 3b, respectively. The universal testing machine (UTM), as presented in Fig. 4, was used to conduct the tensile tests.

Fig. 1 *Gas tungsten arc welding machine*

Fig. 2 *ER316 filler metal*

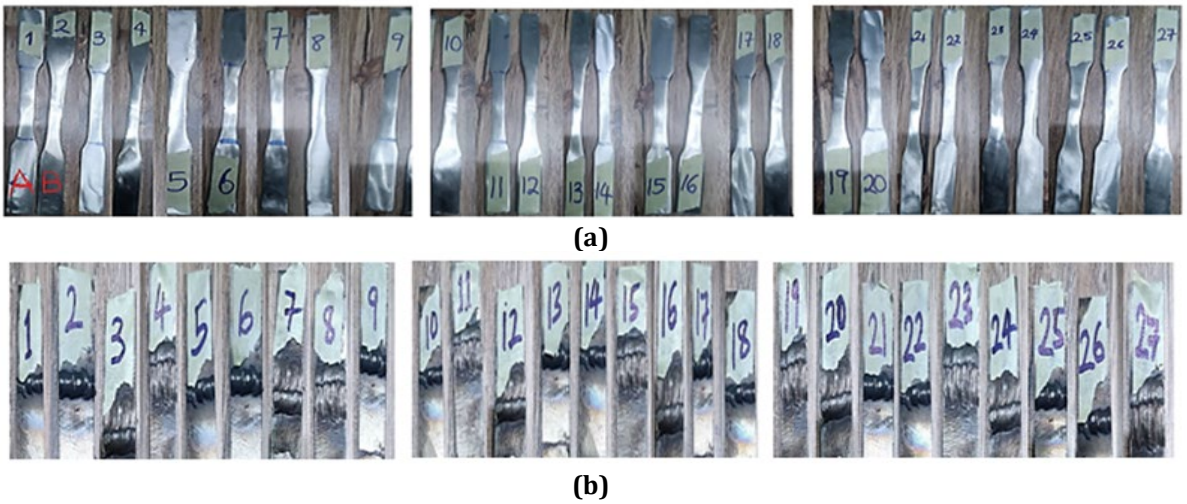

Fig. 3 *Experimental test samples (a) Experimental tensile test samples; and (b) Hardness test samples*

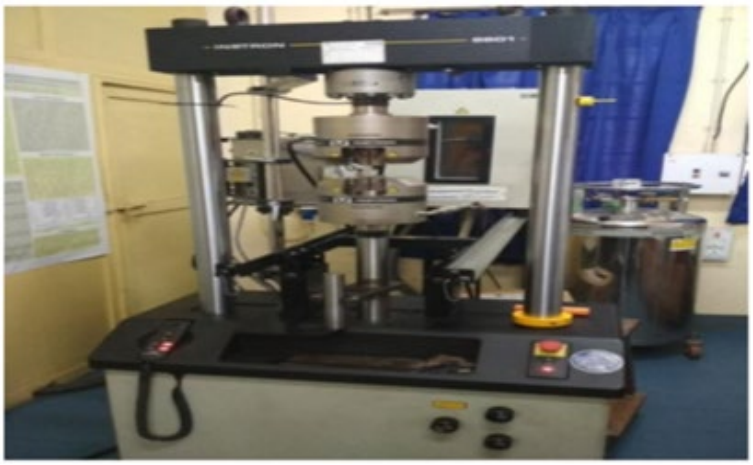

Fig. 4 *Universal tensile test machine*

Table 2 *Elemental composition of the base material and filler material used in this study*

Weight %	C	Cr	Cu	Mn	Mo	Ni	P	S	Si	Fe
AISI 316L	0.026	16.12	0.15	0.97	2.03	10.08	0.043	0.012	0.26	70.31
ERC316L	0.04	18.2	0.75	1.5	2.3	12.0	0.03	0.03	0.45	64.7

Table 3 *Gas tungsten arc welding parameters*

S/N	Welding Parameters	
1	Shielding gas	100% argon
2	Electrode	2% thoriated tungsten
3	Filler rod diameter	3.2 mm
4	Bevel angle	60^{o}
5	Direction of weld	down hand (flat)
6	Electrical characteristic	DCEN (straight polarity)
7	Joint design	Single V-butt
8	Filler metal	ER316L

3.2 Methods

Steel sample plates (250 × 250 ×10 mm) were sectioned longitudinally, cleaned with acetone, and dried to prevent contamination during gas tungsten arc welding.

GTAW parameters are presented in Table 3. The welding joint's edges were ground away to eliminate surface contamination before welding. Additionally, the parts that needed to be joined were meticulously cleaned to remove any paint, dirt, oil, or grease [17]. The bead-on-plate approach was used in the welding process, in which weld beads were placed longitudinally in the centre of each plate in a straight line. Down hand flat position was used during the welding process. Single V-butt joints with an included bevel angle of 60° between AISI 316L steel with a root gap of 2 mm as shown in Fig. 5 were welded by GTA welding using ER 316L filler metal wire. The selected input parameters were employed to fabricate V - butt joints. Cleaning with acetone and using a single V-butt joint design are essential to prevent contamination and ensure consistent weld quality; thereby directly impacting the optimisation of weld parameters and reducing defects like porosity or inclusions.

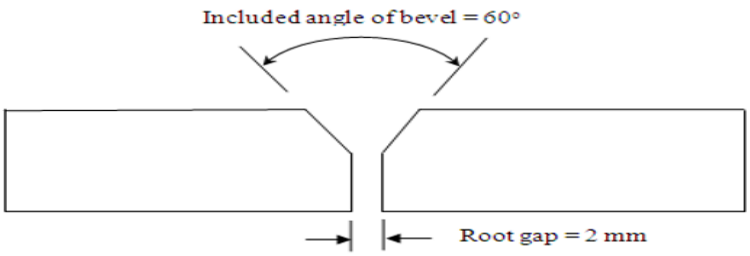

Fig. 5 *Schematic diagram of the joint geometry*

4. Results and Discussion

In this study, tensile strength and microhardness are considered as the quality characteristics of the welding process. The experimental test results, the calculated signal-to-noise ratios, and normalised values are presented in Table 4.

The computed Grey relational coefficient values are displayed in Table 5 which shows the summary of GRGs and their corresponding ranks. From Table 5, Experiment number 11 has the highest value of the Grey relational grades, and hence it was allotted as rank one. The experimental samples and their GRGs are illustrated in Fig. 6. The ideal process parameter setting depicts the relationship between the reference and objective sequences. A higher grey relational grade indicates a stronger association between the two. To achieve higher tensile strength and microhardness in welded specimens, it is best to optimise process parameters with higher GRG. The ideal welding setting is decided based on the highest Grey reasoning grade. Table 6 shows the expected GRC values and accompanying rankings. Table 6 shows that the four welding parameters were optimally adjusted throughout 27 tests. The predicted values of GRC and their corresponding ranks are tabulated in Table 6. The results of Table 6 reveal that among the 27 experiments, the optimal level setting of the four welding parameters for the multiple performance characteristics considered is current at 100 A (medium level), speed is 0.7 mm/s (low level), voltage is 25 V (medium level), and gas flow rate is 20 L/m (high level). As per Table 6, the maximum tensile strength of 653.8 MPa and microhardness of 242.5 HB were obtained.

Table 4 *Calculated normalised values*

Experiment Number	Tensile strength (MPa)	S/N (dB)	Normalised Values	Hardness (HB)	S/N (dB)	Normalised Values
1	565.0	55.0410	0.000	175.8	44.9004	0.0218
2	571.3	55.1373	0.076	174.5	44.8359	0.0000
3	574.4	55.1843	0.113	180.0	45.1055	0.0913
4	587.8	55.3846	0.271	193.8	45.7471	0.3084
5	582.9	55.3119	0.214	196.4	45.8628	0.3476
6	590.5	55.4244	0.302	192.5	45.6886	0.2886
7	596.3	55.5093	0.369	220.3	46.8603	0.6852
8	594.2	55.4787	0.345	222.0	46.9271	0.7078
9	591.8	55.4435	0.317	223.3	46.9778	0.7250

10	647.0	56.2181	0.928	245.2	47.7904	1.0000
11	653.8	56.3089	1.000	242.5	47.6942	0.9674
12	643.7	56.1737	0.8934	244.4	47.7620	0.9904
13	636.4	56.0746	0.8152	218.9	46.8049	0.6664
14	625.1	55.9190	0.6925	220.8	46.8800	0.6919
15	630.6	55.9951	0.7525	217.9	46.7651	0.6530
16	604.8	55.6322	0.4662	221.1	46.8916	0.6958
17	599.5	55.5558	0.4060	219.6	46.8326	0.6758
18	600.0	55.5630	0.4117	222.1	46.9310	0.7091
19	590.7	55.4273	0.3047	210.7	46.4733	0.5542
20	602.3	55.5963	0.4380	212.8	46.5594	0.5833
21	605.6	55.6437	0.4754	209.6	46.4278	0.5388
22	598.3	55.5383	0.3922	219.5	46.8287	0.6745
23	594.4	55.4816	0.3475	219.0	46.8089	0.6678
24	589.6	55.4111	0.2919	220.7	46.8760	0.6905
25	590.1	55.4185	0.2977	217.6	46.7532	0.6489
26	582.9	55.3119	0.2137	218.2	46.7771	0.6570
27	600.2	55.5659	0.4140	219.1	46.8128	0.6691

Table 5 *Computed GRC and GRG Values*

Experiment Number	(GRC)		GRG	Rank
	UTS	Hardness		
1	0.333	0.338	0.1675	27
2	0.351	0.333	0.1719	26
3	0.360	0.355	0.1790	25
4	0.407	0.420	0.2061	23
5	0.389	0.434	0.2035	24
6	0.417	0.413	0.2077	22
7	0.442	0.614	0.2554	14
8	0.433	0.631	0.2561	12
9	0.423	0.645	0.2559	13
10	0.874	1.000	0.4622	2
11	1.000	0.939	0.4878	1
12	0.824	0.981	0.4434	3
13	0.730	0.600	0.3390	4
14	0.619	0.619	0.3095	6
15	0.669	0.590	0.3187	5
16	0.484	0.622	0.2696	7
17	0.457	0.607	0.2585	9
18	0.459	0.632	0.2641	8
19	0.418	0.529	0.2312	21
20	0.471	0.545	0.2503	17

21	0.488	0.520	0.2504	16
22	0.451	0.606	0.2565	11
23	0.434	0.601	0.2504	16
24	0.414	0.618	0.2478	18
25	0.416	0.587	0.2422	19
26	0.389	0.593	0.2353	20
27	0.460	0.602	0.2584	10

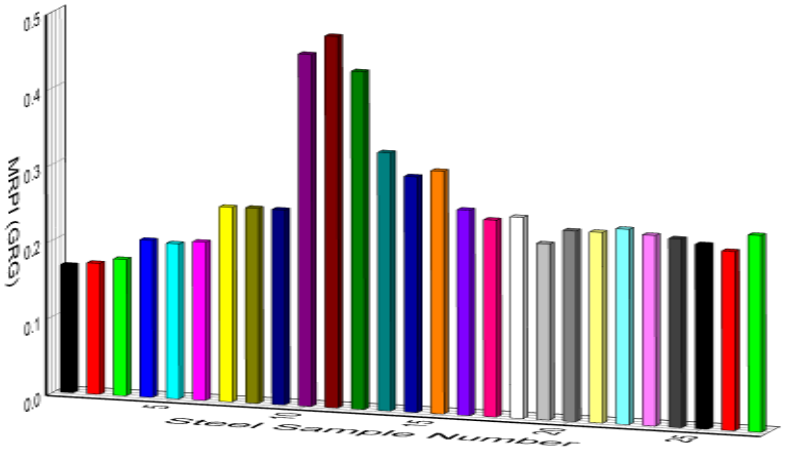

Fig. 6 *Steel sample versus MRPI*

Table 6 *Experimental results based on Taguchi L27 design of experiment*

Experiment Number	J	K	Y	Z	Tensile strength (MPa)	S/N (dB)	Hardness (HB)	S/N (dB)
1	J_1	K_1	L_1	M_1	565.0	55.0410	175.8	44.9004
2	J_1	K_1	L_1	M_1	571.3	55.1373	174.5	44.8359
3	J_1	K_1	L_1	M_1	574.4	55.1843	180.0	45.1055
4	J_1	K_2	L_2	M_2	587.8	55.3846	193.8	45.7471
5	J_1	K_2	L_2	M_2	582.9	55.3119	196.4	45.8628
6	J_1	K_2	L_2	M_2	590.5	55.4244	192.5	45.6886
7	J_1	K_3	L_3	M_3	596.3	55.5093	220.3	46.8603
8	J_1	K_3	L_3	M_3	594.2	55.4787	222.0	46.9271
9	J_1	K_3	L_3	M_3	591.8	55.4435	223.3	46.9778
10	J_2	K_1	L_2	M_3	647.0	56.2181	245.2	47.7904
11	J_2	K_1	L_2	M_3	653.8	56.3089	242.5	47.6942
12	J_2	K_1	L_2	M_3	643.7	56.1737	244.4	47.7620
13	J_2	K_2	L_3	M_1	636.4	56.0746	218.9	46.8049
14	J_2	K_2	L_3	M_1	625.1	55.9190	220.8	46.8800
15	J_2	K_2	L_3	M_1	630.6	55.9951	217.9	46.7651
16	J_2	K_3	L_1	M_2	604.8	55.6322	221.1	46.8916
17	J_2	K_3	L_1	M_2	599.5	55.5558	219.6	46.8326
18	J_2	K_3	L_1	M_2	600.0	55.5630	222.1	46.9310
19	J_3	K_1	L_3	M_2	590.7	55.4273	210.7	46.4733

20	J_3	K_1	L_3	M_2	602.3	55.5963	212.8	46.5594
21	J_3	K_1	L_3	M_2	605.6	55.6437	209.6	46.4278
22	J_3	K_2	L_1	M_3	598.3	55.5383	219.5	46.8287
23	J_3	K_2	L_1	M_3	594.4	55.4816	219.0	46.8089
24	J_3	K_2	L_1	M_3	589.6	55.4111	220.7	46.8760
25	J_3	K_3	L_2	M_1	590.1	55.4185	217.6	46.7532
26	J_3	K_3	L_2	M_1	582.9	55.3119	218.2	46.7771
27	J_3	K_3	L_2	M_1	600.2	55.5659	219.1	46.8128

4.1 Analysis of Experimental Results Using GRG and ANOVA

Table 7 *Mean response table for Grey relational grade*

Level	Mean Grey Relational Grade			
	Current (J) (A)	Speed (K) (mm/s)	Voltage (L) (V)	Gas flow rate (M) (L/min.)
1	0.2115	0.2937	0.2295	0.2468
2	0.3503	0.2599	0.3052	0.2379
3	0.2469	0.2551	0.2741	0.3239
Delta	0.1388	0.0386	0.0757	0.0860
Rank	1	4	3	2
Mean of the total of the GRGs = 0.2696				

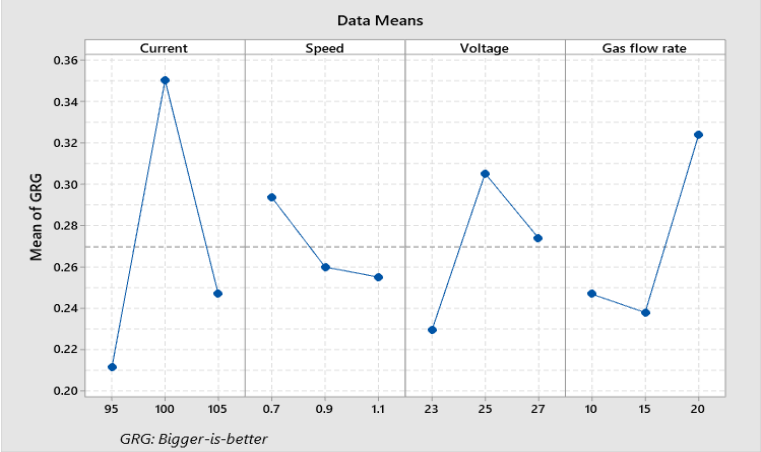

Fig. *7 Main effects plot for Grey relational grades*

This study used Taguchi's orthogonal array to analyse the impact of welding parameters on GRG at various levels. To compute the mean GRG for workpiece welding current at Levels 1 and 2, average the data from Experiments 1-9 and 10-18, respectively. The mean GRG for each level of welding parameters may be determined accordingly. Table 7 presents the mean GRG at each welding parameter level, often known as a response table. The graph depicts the change in reaction as a specific factor moves from Level 1 to 3. The GRG response graph (Fig.7) visualises the impact of welding parameters using Minitab software. The GRG graph depicts how the reaction changes when a factor progresses from Level 1 to 3. The GRG's average response and mean effect plots are vital for analysing the influence of selected process parameters on several performance metrics and establishing the ideal parameter setting. The Taguchi technique defines delta as the difference between the highest and lowest grey relational grades for each parameter. The delta value indicates how the settings affect the process. According to [6], bigger delta values indicate more effect.

Table 7 displays the response table for the means of grey relational grade, and Fig. 7 displays the main effect plots for the grey relational grade analysis, revealing that the major factors influencing tensile strength and microhardness are welding current, followed by gas flow rate, voltage, and welding speed in that order, with the

optimal parameters setting as $J_2K_1L_2M_3$. Level 2 has the biggest effect on factor J in terms of GRG. In factor K, level 1 has the biggest effect on GRG. Level 2 has the greatest effect on GRG in the L component, whereas level 3 has the most influence in the M factor.

Minitab software was used to do an analysis of variance (ANOVA) to determine the relative significance of variables. ANOVA is used to determine which welding factors substantially impact certain performance variables. ANOVA results (Table 8) show that welding current is the most significant welding parameter affecting multiple response performance index (MRPI), with a percentage contribution of 58.31%. This aligns with the results from the mean response table (Table 7). Variations in welding current influence heat input, penetration depth, and weld pool dynamics. For example, higher currents lead to deeper penetration and slower cooling rates, which enhance joint strength but risk defects like grain coarsening. Figure 8 displays the percentage contribution of the various welding parameters to MRPI. Hence from the ANOVA results obtained, it can be used to guide parameter adjustments in real-world applications, emphasising the statistical significance of key parameters like current and shielding gas flow rate in the welding operation of austenitic stainless steel.

Table 8 *Analysis of variance (General Linear Model): GRG versus current, speed, voltage, gas flow rate*

Source	DF	Seq SS	Contribution	Adj SS	Adj MS	F-Value
Current	2	0.093675	55.05%	0.093675	0.046837	391.61
Speed	2	0.007995	4.70%	0.007995	0.003998	33.42
Voltage	2	0.026059	15.32%	0.026059	0.013029	108.94
Gas flow rate	2	0.040270	23.67%	0.040270	0.020135	168.35
Error	18	0.002153	1.27%	0.002153	0.000120	
Total	26	0.170152	100.00%			

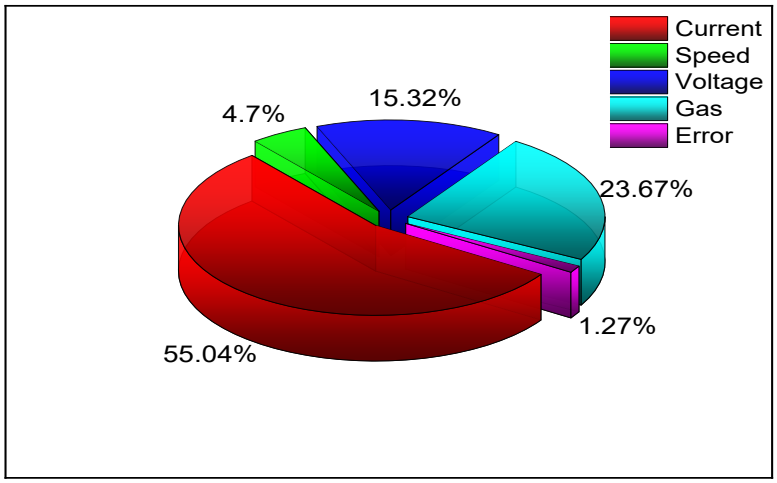

Fig. 8 *Percentage contribution of welding parameters*

4.2 Effect of Process Parameters on Tensile Properties

Table 9 illustrates how welding settings affect tensile strength and microhardness. Using Origin Pro software, Fig. 9 (a) - (d) illustrates how welding factors such as current, speed, voltage, and gas flow rate affect tensile strength (UTS) and microhardness. The welded joint's UTS varied from 583.8 to 626.8 MPa, with microhardness ranging from 197.2 to 257.8 MPa.

In Fig. 9(a), increasing the welding current leads to a rise in tensile strength and microhardness, ultimately reaching the optimal value. Welding current significantly affects the mechanical characteristics of welded joints. For instance, higher heat input can lead to grain coarsening, reducing hardness, while optimal heat minimises carbide formation and maintains corrosion resistance (18-21). Fig. 9(b) indicates that increasing welding voltage leads to an increase in tensile strength and microhardness, followed by a decrease in tensile characteristics. Plots 9(c) and 9(d) demonstrate that welding speed and gas flow rate have comparable impacts on the tensile and hardness parameters of a steel welded joint. As traverse speed rises, tensile characteristics decrease because of grain coarsening caused by inadequate heat for dynamic recovery and recrystallisation. Increased speeds minimise heat input per unit length, resulting in smaller fusion zones. Welding productivity relies heavily on

traverse speed. Setting the traverse speed too low can lead to material deterioration from arc heat and over-deposition. Traverse speed is not a desirable parameter for controlling mechanical qualities.

Clearly, from Fig. 9(d), it is seen that there is an increasing trend in microhardness as gas flow rate Increases, arising perhaps from less surface contamination in the weld pool resulting from greater protection from atmospheric contamination via the higher flow rate of shielding gas. It can be inferred that increasing the shielding gas flow rate can reduce porosity and improve tensile strength. As expected the lowest tensile strength and microhardness were obtained when the welded joint was not sufficiently shielded during welding.

Table 9 *Variation of tensile strength and microhardness with welding parameters*

Parameter	Average Tensile Strength (MPa)	Average Microhardness (HB)
Welding Current		
Level 1	583.8	197.2
Level 2	626.8	228.1
Level 3	594.5	216.4
Welding Speed		
Level 1	606.0	210.6
Level 2	604.0	211.1
Level 3	595.5	220.4
Voltage		
Level 1	588.6	205.8
Level 2	608.8	218.9
Level 3	608.1	217.4
Gas Flowrate		
Level 1	597.3	204.8
Level 2	596.0	257.8
Level 3	612.1	228.5

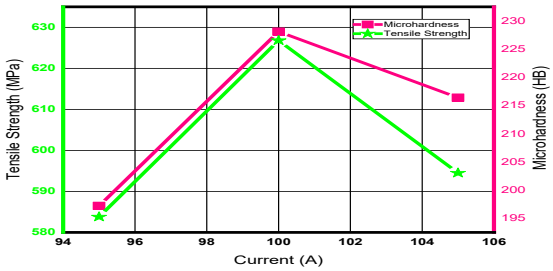

Fig. 9 (a) *UTS, microhardness versus current*

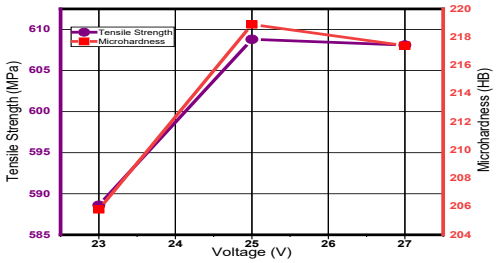

Fig. 9 (b) *UTS, microhardness versus voltage*

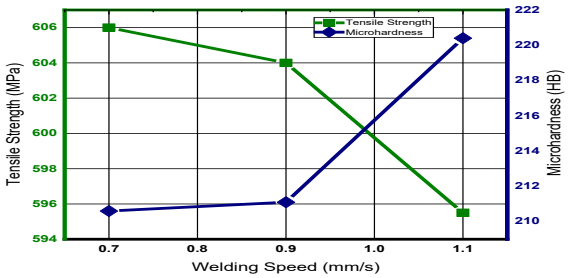

Fig. 9 (c) *UTS, microhardness versus speed*

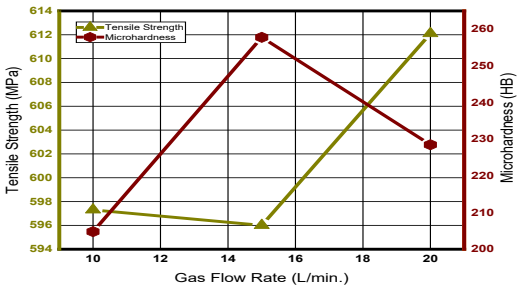

Fig. 9 (d) *UTS, microhardness versus gas flowrate*

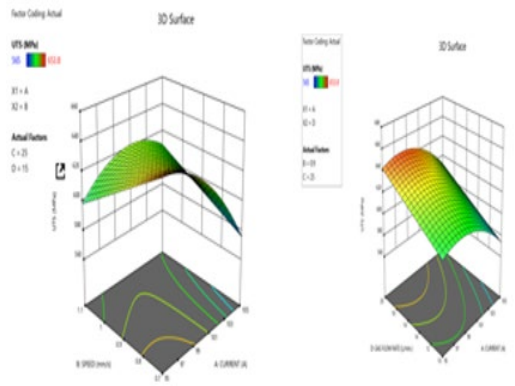

Fig. 10 *(a) Speed, current vs. UTS; (b) GFR, current vs. UTS*

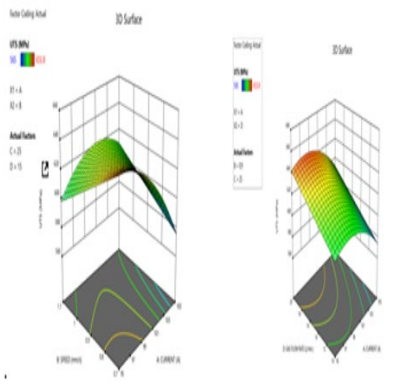

Fig. 11 *(a) voltage, current vs. UTS; (b) Speed, GFR vs. UTS*

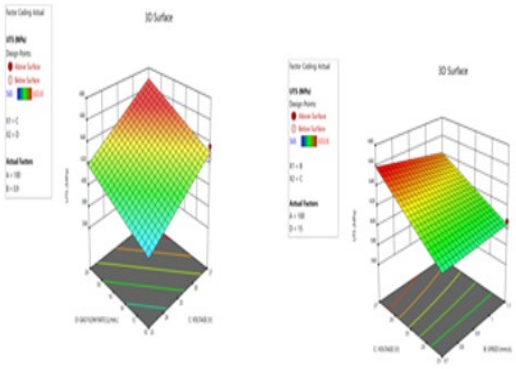

Fig. 12 *(a) GFR, voltage vs. UTS; (b) Voltage, speed vs. UTS*

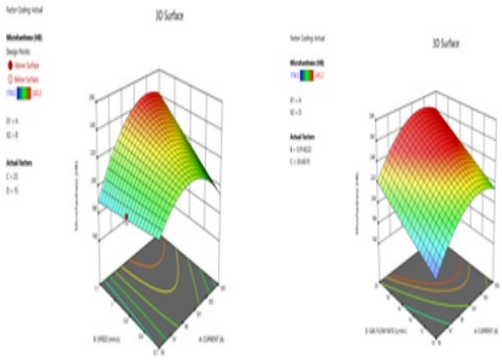

Fig. 13 *(a) Speed, current vs. hardness; (b) GFR, current vs. hardness*

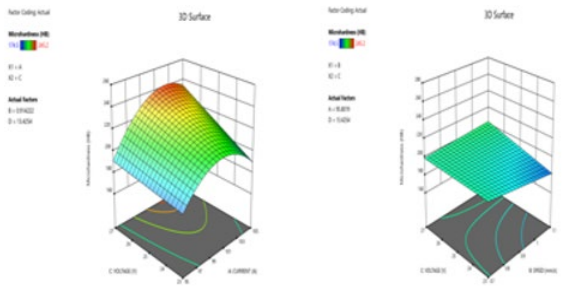

Fig. 14 *(a) Voltage, current vs. hardness; (b) Voltage, speed vs. hardness*

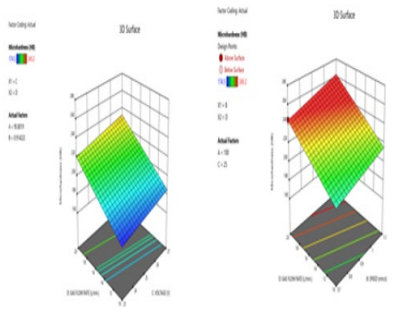

Fig. 15 *(a) Voltage, GFR vs. hardnesS; (b) GFR, speed vs. hardness*

Design Expert computer software created 3D surface and contour plots of Figs. 10 - 15, which demonstrate the combined impacts of two welding parameters vs. UTS and microhardness, respectively. Fig. 10(a) shows that tensile strength improves as current and welding speed drop, implying that tensile strength increases at low heat inputs. Tensile strength is also reduced at high current and low welding speed, implying that at low speed and high current, the grains coarsen, leading to low tensile strength.

From Fig. 10(b), at a low gas flow rate, porosity in the weld may occur perhaps from atmospheric contamination resulting from insufficient protection from the shielding gas, and at high current, it leads to a reduction in tensile strength, which is consistent with [16] earlier findings. On the other hand, sufficient shielding gas at low heat input results in improved tensile strength. As shown in Fig. 11(a), the tensile strength of a weld increases as the voltage rises and the current decreases. The plots in Fig. 11(b) show that welding speed has only

a barely perceptible effect on UTS, whereas UTS increases as the gas flow rate increases. It is obvious from the surface plots in Fig. 12(a) that there is a steady and steep rise in tensile strength as both voltage and gas flow rate increase in value, an indication that both voltage and gas flow rate have a significant impact on the tensile strength of the welded joint. From Fig. 12(b), the relationship trend of speed and voltage with UTS is similar to that in Fig. 11(b) of speed and gas flow rate with UTS.

As regards the combined impact of current and welding speed on microhardness, Fig. 13(a) reveals that maximum UTS was obtained at high welding speed and medium current, resulting in optimum tensile properties of the weld. The plots of Fig. 13(b) indicate that as both gas flow rate and current increase, microhardness increases. Increasing current increases heat input, leading to coarser microstructure and lower hardness. Higher currents can also lead to increased penetration, potentially improving hardness. On the other hand, increasing the gas flow rate reduces hardness due to increased cooling rates and reduced heat input. Therefore, it can be argued that the higher cooling rate of the high gas flow rate moderated the high heat input achieved due to the high current supplied, resulting in the optimal hardness levels observed in the weld. Fig. 14(a) shows that moderate levels of voltage and current produced optimal hardness and microstructure in the steel weld. The graphs of Fig. 14(b) indicate that the combined effect of higher voltage and slower welding speed culminated in lower hardness, with marginal changes thereafter. It is obvious from Fig. 15(a) that the combined effect of gas flow rate and voltage is that a higher gas flow rate and lower voltage produced higher hardness. Conversely, lower gas flow rate and higher voltage resulted in lower hardness.

Furthermore, the combined influence of gas flow rate and welding speed on the microhardness of 316L austenitic stainless steel weld is highlighted in Fig. 15(b); higher hardness is achieved at higher gas flow rates and faster welding speeds, while lower gas flow rates and slower welding speeds produce lower hardness.

4.3 Confirmatory Test

Ultimately what remains is the prediction, verification, and experimental validation of the optimisation of the GTAW process parameters of 316L austenitic stainless steel. The value of the calculated or predicted GRG, using the maximum levels of the welding process parameters is derived from Equation 6 [22].

$$\mathrm{M} = \mathrm{M_a} + \sum_{j=1}^{n}(M_r - \mathrm{M_a}) \tag{6}$$

Where N is the calculated or predicted GRG
$\mathrm{M_a}$ is the average or mean of the total of the GRGs of all the runs,
M_r is the average of the GRGs at the required level of the process parameters,
and n = is the relevant welding process parameters of the GRG.

Table 10 *Validation test table*

	Initial levels of welding parameters	Optimal levels of welding parameters	
	Experiment	Prediction	Experiment
Level Combination	$J_1K_1L_1M_1$	$J_2K_1L_2M_3$	$J_2K_1L_2M_3$
Tensile strength	573.2		657.3
Hardness	183.7		243.8
GRG	0.0409	0.417	0.495
Improvement in reasoning		0.3761	0.4541

However, the Taguchi-Grey optimised values were confirmed by GTAW welding testing with the same input variables, conditions, and limitations as in the modelling procedure, yielding a maximum UTS of 657.3 MPa and a maximum microhardness of 243.8 HB. The slight discrepancy might have been attributable to unaccounted-for flaws in the experimental technique. Thus, a confirmatory experiment was carried out utilising the optimal values of the GTA welding parameters acquired from the Grey relational analysis, and the GRG was computed or projected using Equation (6), to check and validate the improvement in the multiple response performance index. Table 10 illustrates the projected and actual GRG values, which have increased from 0.0409 to 0.495. Therefore, arising from the result of the confirmatory experiment, the desired optimal combination of welding parameters was $J_2K_1L_2M_3$. Incidental experimental errors such as gas flow rate fluctuations or equipment variability, could account for the discrepancy observed between the predicted and actual experimental results, and the use of automated welding setups could help to minimise them. There is a 20.7% difference in improvement between the predicted and actual results indicating that the model is reliable. However a higher volume of confirmatory experiments could average out experimental error effects thereby resulting in enhanced performance of the model.

5. Conclusion

The study's findings have proven the Taguchi-Grey optimisation technique to be an effective and reliable predictive model for optimising welding parameters for high-quality welds and enhanced mechanical performance of austenitic stainless steel. This optimisation technique could be applied in aluminum welding in automotive manufacturing or titanium in aerospace industry. This model could perhaps be deployed in other materials such as composites or multi-objective engineering applications.

Acknowledgement

Communication of this research is made possible through monetary assistance by Universiti Tun Hussein Onn Malaysia and the UTHM Publisher's Office via Publication Fund E15216.

Conflict of Interest

Authors declare that there is no conflict of interests regarding the publication of the paper.

Author Contribution

The authors confirm contribution to the paper as follows: ***study conception and design****: Afabor A. M.;* ***data collection****: Afabor A. M.;* ***analysis and interpretation of results****: Onyekpe B. O., Awheme O.;* ***draft manuscript preparation****: Afabor A. M., Awheme O.; All authors reviewed the results and approved the final version of the manuscript.*

References

[1] Khubaib Z. G.; A. Sadaqat; U. D. Emad; M. Aamir; B. K. Niaz and W. A. Syed (2022). Experimental investigation of the effect of welding parameters on surface roughness, micro-hardness, and tensile strength of AISI 316L stainless steel welded joints using 308L filler material by TIG welding. Journal of Materials Research and Technology, Vol.21: 220 – 236

[2] Piyush K. G, and Abhishek K. (2017). SMAW process parameters optimisation using Taguchi and Fuzzy Logic. International Research Journal of Engineering and Technology, Volume 04 Issue 05, pp. 411-413.

[3] Thakur P.M. and Rajesh R. (2014). Optimal selection of process parameters in CNC end milling of Al 7075-T6 aluminium alloy using a Taguchi-Fuzzy approach. Proceedia Materials Science 5: 2493 – 2502

[4] [Girish B. M.; H. S. Siddesh and B. M. Satish (2019). Taguchi grey relational analysis for parametric optimisation of severe plastic deformation process. Springer Nature Applied Sciences 1:937 https://doi.org/10.1007/s42452-019-0982-6

[5] Xuelong Wang (2019). Application of grey relation analysis theory to choose high reliability of the network node. Journal of Physics: Conf. Series 1237 (2019) 032056 doi:10.1088/1742-6596/1237/3/032056

[6] Argha D.; M. Arindam and K. D. Pankaj (2014). Detection of apposite PSO parameters using Taguchi based Grey relational analysis: optimisation and implementation aspects on manufacturing related problem. 3rd International Conference on Materials Processing and Characterisation.

[7] Shaiful Fadzil Zainal Abidin, Mohamad Helmi Ripin, Rifqi Irzuan Abdul Jalal, Nurulafiqah Aziz (2024). Optimising gear ratios for vehicle performance enhancement using Taguchi method. Journal of Advanced Industrial Technology and Application, Vol. 5 No. 1, 11-20

[8] Glauco N.; S. S, Maria; R. M. Manuel; R. G. Pablo and R. João (2021). Parametric optimisation of the GMA welding process in thin thickness of austenitic stainless steel by Taguchi method. Appl. Sci. Vol. 11(18), pp. 42-87.

[9] Afabor Abraham Martins and Ikikiru Diatachekor Friday (2022). Parametric optimisation of gas tungsten arc welding on the tensile strength of AISI 316L austenitic stainless steel using Taguchi method. Journal of Materials Engineering, Structures and Computation 1(1), pp. 90-101

[10] Subodh Kumar and A.S. Shahi (2011). Effect of heat input on the microstructure and mechanical properties of gas tungsten arc welded AISI 304 stainless steel joints. Materials and Design 32, 3617–3623

[11] Wichan Chuaiphan and Loeshpahn Srijaroenpramong (2020). Microstructure, mechanical properties and pitting corrosion of TIG weld joints alternative low-cost austenitic stainless steel grade 216. Journal of Advanced Joining Processes 2 (2020) 100027 https://doi.org/10.1016/j.jajp.2020.100027

[12] Sri W. and Sapto W. I. (2018). Application of multi response optimisation with grey relational analysis and fuzzy logic method. J. Phys.: Conf. Ser. 948 012075 doi:10.1088/1742-6596/948/1/012075

[13] Mahiratul Husna Mustaffar and Aliff Hisyam A. Razak (2021). Optimisation of tensile strength and weight loss via Taguchi and response surface method for natural rubber latex film consisting cassava peel as a bio-based filler. Journal of Advanced Industrial Technology and Application, Vol. 2 No. 1, 7-17

[14] Vijayan D. and Seshagiri R. V. (2017). Optimisation of friction stir welding process parameters using RSM based Grey–Fuzzy approach. Saudi Journal of Engineering Technology, Vol-2, issue 1, pp. 12-25
[15] Hsuan-Liang L. and You-Jiun W. (2021). Optimisation of the MIG arc weld-brazing process on titanium and aluminum lap-joint welds using the Taguchi method, grey relational analysis and fuzzy logic. The International Journal of Advanced Manufacturing Technology doi: https://doi.org/10.21203/rs.3.rs-443418/v1
[16] Szwajka K.; J. Zielin´skaSzwajka and T. Trzepiecin´ski (2024). The Influence of the Shielding-Gas Flow Rate on the Mechanical Properties of TIG-Welded Butt Joints of Commercially Pure Grade 1 Titanium. Materials, 17, 1217. https:// doi.org/10.3390/ma17051217
[17] Benjamin Ufuoma Oreko and Silas Oseme Okuma (2024). The Influence of post-weld tempering on the mechanical and microstructural behaviour of AISI 1040 carbon steel weld. Journal of Advanced Industrial Technology and Application, Vol. 5 No. 1, 57-65
[18] Adzor, S.A., Afabor, A.M., Pullah, A. and Utu, O.G. (2023). Optimisation of welding and heat treatment parameters for enhanced mechanical performance in micro-alloyed steel components. Nigerian Research Journal of Engineering and Environmental Sciences, 8(2), pp. 347-358
[19] Kayode, Joseph; Akinola, Adebisi Olayinka and Akinwekomi, Akeem Damilola (2020). Effects of bevel angle and heat input on tensile property and microstructures of mild steel weldments. Annals of Faculty of Engineering Hunedoara – International Journal of Engineering, Vol.18, pp. 33-38.
[20] Sutrimo Ating Sudradjat, Rayhan Nugraha, Fachri Koeshardono, Aris Suryadi, Deni Mulyana and Ita Casmita (2019). Effect of heat input variations to the mechanical properties and pitting corrosion in the dissimilar stainless-steel welding. International Journal of Advances in Scientific Research and Engineering (ijasre), Volume 5, Issue 10, pp. 115-123. DOI: 10.31695/IJASRE.2019.33541
[21] Mosa, E. S., Morsy, M. A. and Atlam A. Effect of heat input and shielding gas on microstructure and mechanical properties of austenitic stainless steel 304L. International Research Journal of Engineering and Technology (IRJET) Volume: 04 Issue: 12, pp. 370-377
[22] Jenarthanan M.P. and Jeyapaul R. (2015). Analysis and optimisation of machinability behaviour of CFRP composites using fuzzy logic. Pigment & Resin Technology Volume 44, Number 1, 48–55